HHS Public Access

Author manuscript

OpenNano. Author manuscript; available in PMC 2025 May 08.

Published in final edited form as:

OpenNano. 2025 January ; 21: . doi:10.1016/j.onano.2024.100223.

Bioprinting 3D lattice-structured lumens using polyethylene glycol diacrylate (PEGDA) combined with self-assembling peptide nanofibers as hybrid bioinks for anchorage dependent cells

Vishalakshi Irukuvarjula,
Faye Fouladgar,
Robert Powell,
Emily Carney,
Neda Habibi*

Department of Biomedical Engineering, University of North Texas, Denton, TX, United States

Abstract

There is a pressing need for new cell-laden, printable bioinks to mimic stiffer tissues such as cartilage, fibrotic tissue and bone. PEGDA monomers are bioinks that crosslink with light to form a viscoelastic solid, however, they lack cell adhesion properties. Here, we utilized a hybrid bioink by combining self-assembled peptide nanofibers with PEGDA for 3D printing lumens. Adult human dermal fibroblast (aHDF) cells were first seeded in peptide-laden in 2D and 3D layers and cell behavior were studied. The cell's morphology remained spheres when they were infused in the 3D hydrogel and highly aligned with 2D overlay hydrogels. HDF cells did not adhere to unmodified PEGDA lumens, however, they successfully attached and proliferated on PEGDA/peptide lumens. Moreover, HDF cells seeded on the hybrid PEGDA/peptide lumens displayed a distinct spread F-actin morphology. The results showcase the potential of peptide hydrogels in facilitating interaction of anchorage dependent cells with PEGDA structures.

Keywords

PEGDA; Lumens; Self-assembling peptides; 3D bioprinting; Human dermal fibroblast cells

*Correspondence author at: Department of Biomedical Engineering, University of North Texas, Denton, TX, United States. neda.habibi@unt.edu (N. Habibi).

Declaration of competing interest

The authors declare that they have no known competing financial interests or personal relationships that could have appeared to influence the work reported in this paper.

CRediT authorship contribution statement

Vishalakshi Irukuvarjula: Data curation, Investigation, Methodology, Project administration. **Faye Fouladgar:** Data curation, Methodology. **Robert Powell:** Data curation, Investigation, Methodology. **Emily Carney:** Data curation. **Neda Habibi:** Conceptualization, Funding acquisition, Investigation, Methodology, Resources, Supervision, Validation, Writing – original draft, Writing – review & editing.

1. Introduction

In the past decade, 3D bioprinting has become a valuable method for creating customized patient-specific tissue structures [1]. This process involves layering biologically derived materials or cells to build tissue [2,3]. There are different approaches to bioprinting, generally divided into two categories: printing without cells (acellular printing) and adding them later, or directly printing with cells in a "bioink." The three main types of bioprinting techniques are droplet-based, extrusion-based [4,5] and light-based bioprinting [6–8]. Each of the bioprinting technique offers unique benefits, however, the light-based methods stand out for their ability to achieve high throughput and high-resolution features [9].

In photocuring-based bioprinting, photosensitive polymers are solidified to create constructions under carefully regulated light that may be printed quickly and precisely [10,11]. Due to various light scanning technologies, it may also be divided into projection-based printing (also known as. digital light processing, or DLP) and stereolithography (SLA). The advantages of photocuring-based bioprinting include excellent resolution and zero nozzles, when compared to all other 3D printing methods. These structures can accommodate high resolution feature, and channels such as branching and tapering vessels that have significant potential in applications such as lab-on-a-chip devices, microfluidics, cell-laden hydrogels, and tissue engineering [12].

Recent advancements in 3D bioprinting (i.e., 3D printing with cells) have sparked significant enthusiasm for its potential in producing transplantable tissues. However, to date, proof-of-concept studies have been largely confined to architecturally simple tissues, such as skin and cardiac patches [13]. A key challenge has been the limited availability of bioinks [14] that possess both the necessary properties for 3D bioprinting of complex tissues and the specific biological signals required to promote tissue maturation both in vitro and in vivo [15]. For instance, Polyethylene glycol diacrylate (PEGDA) is a frequently utilized bioink in DLP bioprinter [16], wherein the monomers are crosslinked to form the final gel. Although PEGDA is advantageous for its photopolymerization capabilities, it lacks inherent cell adhesion properties [17]. Consequently, a significant challenge in advancing this technology for tissue engineering involves modifying the bioinks to enhance cell adhesion, proliferation, and growth [18]. Few strategies have been investigated to enhancing the biological activity of engineered materials and bioinks, including the incorporation of specific ligands, individual extracellular matrix (ECM) components [19], or surface modifications to improve cell adhesion and vascularization. However, these approaches typically target enhancing biological activity at a single stage of tissue development, such as promoting cell attachment or utilizing growth factors to encourage vascularization. Supporting the various stages required to create functional engineered tissue necessitates multiple biological components and signals that must be precisely coordinated in both space and time. Here, we introduce the development of a novel class of tissue-specific hybrid bioinks, using PEGDA modified with self-assembling short di-peptides based on Phenylalanine-Phenylalanine (FF) hydrogels [20]. Supramolecular hydrogelators made from short peptides offer several benefits over traditional polymeric hydrogels: (i) they have a clear and defined arrangement and structure [21]; (ii) they are generally more biocompatible and biodegradable due to the non-covalent interactions between molecules [22]; and (iii) they more closely resemble the extracellular

matrix (ECM) since the self-assembled nanostructures typically range from 5 to 300 nm (iv) they have shown to promote differentiation in various cells including mesenchymal stem cells [23]. To leverage the bioactivity of FF peptides, we first seeded adult human dermal fibroblast (aHDF) in Fmoc-FF hydrogel and observed how HDF cells responded to the peptide's microenvironment in terms cell adhesion and cell-material interaction. Further, a honeycomb lattice lumen was printed by combing PEGDA bioinks with peptides during printing or coating them with peptides after printing. We investigated the capability of modified scaffolds to support cell adhesion, proliferation and expanding using dermal fibroblast cells. The results showcase the potential of peptide hydrogels in facilitating interaction of anchorage dependent cells with PEGDA lumen structures.

2. Materials and methods

2.1. Materials

Adult Human Dermal Fibroblast cell line (aHDF; catalog no – C0135C) was acquired from Thermo Fisher Scientific, USA, as a cryopreserved vial and eventually stored in a liquid nitrogen tank before use. The cells were maintained in growth medium Dulbecco's Modified Eagle Medium (DMEM catalog no – 11,995,065) which was supplemented with certified Fetal Bovine Serum (FBS; catalog no 16,000,069) and antibiotics, all were purchased from Thermo Fisher Scientific. Trypsin-EDTA, l-Phenylalanyl-l-phenylalanine (Phe-Phe catalog no J60043.03), Fmoc-Phe-Phe were also obtained from Thermo Fisher Scientific. Hexafluoroisopropanol (HFP/1,1,1,3,3,3-Hexafluoro-2-propano catalog no 105,228) was obtained from Millipore Sigma. Matrigel® Matrix was obtained from Fisher Scientific (catalog no – CB-40,234, Corning USA). The PEGDA Photoink and LumenX+ DLP Bioprinter were purchased from CELLINK A BICO Company, Gothenburg, Sweden.

2.2. Adult human dermal fibroblast (aHDF) cell culture

The aHDF was obtained from Thermo Fisher Scientific, USA. The cells were cultured in Dulbecco's Modified Eagle Medium (DMEM) supplemented with 1 % antibiotics (penicillin and streptomycin) and 10 % Fetal Bovine Serum (FBS). The cells were maintained at 37°C in a humidified chamber i.e. an incubator containing 5 % CO2. The cell culture medium was replaced every 2 days. Cells upon reaching 85 %– 90 % confluency, they were trypsinized using Trypsin-EDTA and cells were subjected to cell passaging.

2.3. Phe-Phe peptide hydrogels synthesis

Fmoc-Phe-phe and Phe-Phe from Thermo Fisher Scientific, USA was used to prepare the peptide nanofibers and hydrogels. HFP (Hexafluoroisopropanol) was used to dissolve peptides. The stock solution was prepared at a concentration of 100 mg/ml. This stock solution was subjected to vortexing and ultrasonication until all the aggregates get dissolved and form a clear solution. Subsequently, the stock solution was diluted to a final concentration of 20 mM (20 μl) in 1 ml of sterile distilled water [21]. Fmoc-Phe-Phe resulted in gel formation and Phe-Phe results in nanofibers.

2.4. Rheological measurements of peptide hydrogels and PEGD/peptide lumens

To evaluate the physical properties of the peptide hydrogels, amplitude sweeps, and viscosity tests were conducted using a parallel plate rheometer (Anton Paar MCR92). Peptide hydrogels 2 % in DMSO and HFP were tested with a 25 mm parallel plate (PP-25). Amplitude sweeps, comprising 21 data points, were performed at shear strains ranging from 0.01 % to 100 %, with a constant angular frequency of 10 rad/s and a force-controlled profile set to 0.1 N. This force-controlled approach ensured consistency between samples despite minor height variations, rather than relying on a fixed gap setting.

2.5. Cell-laden of aHDF cell with FF-based peptides

HDF were first seeded in Fmoc-FF hydrogels with various approaches. In surface-coated hydrogel, peptide hydrogel is coated on the petri dish, and cells are seeded on top (2D cell culture).

In the “Overlay Hydrogel” approach, peptide hydrogel is coated on top of the seeded cells (2D cell culture). In the “Infused Hydrogel”, cells are infused within the peptide hydrogel (3D cell culture). Peptide were diluted in growth medium instead of water to develop the gels, and the infused hydrogel/cell was kept in cell inserts. The medium for all condition were changed every 2 days. Cells were cultured for 5 days and were subjected to MTT, and LIVE-DEAD (viability assay), F-actin (Cytoplasm) and DAPI (nucleus) staining.

2.6. Modifying PEGDA bioink with FF peptides

L-Phenylalanyl-l-phenylalanine (Phe-Phe), was incorporated into PEGDA bioink. The peptide synthesis and modification followed an established protocol. Hexafluoroisopropanol (HFP) was used to dissolve the dipeptides, creating a stock solution with a concentration of 100 mg/ml (0.01 g in 100 μl of HFP). The solution was vortexed and ultrasonicated until all aggregates were fully dissolved, forming a clear solution. This stock was then diluted to a final concentration of 20 mM (20 μl) in 1 ml of PEGDA bioink. To protect the light-sensitive bioink, the solution was wrapped in aluminum foil and maintained at 20 °C in a sterilized environment.

2.7. Bioprinting of Lumen lattice constructs with Lumen X

The Lumen $X+$ 3D Bioprinter (CELLINK, A Bico Company, Gothenburg, Sweden) was used to fabricate high-resolution structures utilizing digital light processing (DLP) technology. The printing process involves light projected through bioinks onto a PDMS-coated petri dish, solidifying the material in an inverted manner. The platform elevates by 100 μm after each layer is printed, with each subsequent layer adhering through light exposure. Polyethylene glycol diacrylate (PEGDA) bioinks were used in this multilayer printing process (Fig. 1).

Three different types of lumen lattice constructs were fabricated: (1) Matrigel-coated, (2) peptide-coated, and (3) peptide-infused lumen lattices. The bioprinter specifications included a 405 nm light wavelength, 50 μm pixel resolution, 5 μm z-axis precision, a projected image size of 1280 × 800 pixels, and an adjustable print bed heating range of 35 °C to 75 °C (Fig. 1). Printing parameters were as follow: Layer thickness 100, burn in factor

(4x), exposure time (18s), and light projection power (48 %). The entire printing process was conducted within a biosafety cabinet to ensure sterility. After printing, the constructs were carefully removed from the build platform and rinsed twice with sterile water. The lumen lattices were then soaked in water for 15–20 min to eliminate any unlinked bioink residues, followed by a single PBS wash. The scaffolds were subsequently transferred to 12-well plates for post-printing modifications and cell culture preparation.

2.8. Post-Printing modification of lumen structures with Phe-Phe and matrigel

Lumen constructs were coated with dipeptide hydrogel to investigate cell behavior, adhesion, migration, and proliferation. The surface was treated with 300–100 μl of diluted peptide solution and allowed to air dry overnight in a sterile biosafety cabinet. After drying, constructs were rinsed with PBS, followed by the addition of 1.5 ml growth medium and a 24-hour incubation for conditioning prior to cell culturing. The same procedure was used to coat Matrigel on the Lumens.

2.9. LIVE/DEAD cell viability assays

Live-Dead" assay was conducted using the LIVE/DEAD Viability/Cytotoxicity Kit to assess cell viability. Cells were treated with Calcein-AM (staining live cells green) and Ethidium homodimer-1 (staining dead cells red) for 30 min at room temperature. Fluorescence microscopy was used for imaging. All experiments were performed in triplicate to ensure accuracy and reliability.

2.10. Cytoplasm phalloidin and nucleus DAPI staining

To assess cellular behavior on scaffolds, F-actin and DAPI staining were performed on day 4 of cell culture. The lumen lattice was fixed with 4 % paraformaldehyde for 15 min, followed by permeabilization with 0.1 % Triton X-100 for 10 min. After washing with PBS, cells were blocked with 1 % BSA for one hour. DAPI and phalloidin were used to stain nuclei and F-actin, respectively. Following 24-hour incubation, the cells were washed with PBS and imaged using a fluorescence microscope. All experiments were conducted in triplicate to ensure accuracy and reliability.

2.11. MTT cell proliferation assay

The MTT assay was used to assess cell viability by quantifying the metabolic activity of cells. Cells were seeded onto scaffolds and incubated for a specified period. After incubation, MTT reagent (3-(4,5-dimethylthiazol-2-yl)–2,5-diphenyltetrazolium bromide) was added to the wells and allowed to react with active mitochondrial enzymes in viable cells, reducing the yellow MTT to purple formazan crystals. The formazan was then solubilized using a detergent solution, and the absorbance was measured at 570 nm using a spectrophotometer. Higher absorbance values indicate greater cell viability and metabolic activity [24].

2.12. Scanning electron microscopy

FF nanofibers deposited on silicone substrates were imaged using scanning electron microscopy (SEM) to analyze surface morphology and structural features. They were

then sputter-coated with a thin layer of gold to enhance conductivity. SEM imaging was performed at an accelerating voltage of 5–10 kV, allowing for high-resolution visualization of the Fmoc-FF hydrogel structures and their interaction with the silicone surface.

2.13. Statistical analysis

was performed in GraphPad Prism and Excel XL toolbox NG using one-way ANOVA and *t*-test. P value <0.05 is considered significant. Each experiment was repeated with 3 technical replicates per experiment.

3. Results and discussion

3.1. Rheological properties of Fmoc-FF in DMSO and HFP

Peptide hydrogels were formed using a 2 % Fmoc-FF in DMSO and HFIP. The gelation process was rapid, with gels forming immediately after mixing, followed by stirring for an hour and allowing the gels to solidify for 24 h. After this period, the gels maintained their 3D structure for several days, demonstrating structural integrity. Rheological characterization was conducted using parallel plate rheology to compare the storage modulus (G') of the hybrid hydrogels within the linear viscoelastic region (LVR). For these tests, we employed an oscillatory measurement with an amplitude sweep. The storage and loss moduli of the Fmoc-FF hydrogels were measured, revealing that the samples exhibited viscoelastic properties with both solid and liquid characteristics. The storage modulus of the Fmoc-FF gels dissolved in DMSO was approximately 80 Pa (Fig. 2a), while the Fmoc-FF dissolved in HFIP exhibited a slightly higher storage modulus of around 100 Pa (Fig. 2b). The higher stiffness observed in the Fmoc-FF gels dissolved in HFIP suggests that this solvent promotes a more robust assembled state, leading to enhanced mechanical properties. These findings align with previous studies, indicating that the choice of organic solvent used to dissolve Fmoc-FF peptides significantly impacts the resulting gel assemblies [21,25]. While ability to produce hydrogels with varying stiffness is of particular importance in regenerative medicine and 3D cell culture applications, the hydrogel should remain printable. The stiffness should be adjusted in a way that the hydrogel remain their integrity with printing forces, however do not prevent printing [26]. In addition, optimal scaffold stiffness, typically measured as Young's modulus, must mimic the native tissue's mechanical properties to provide appropriate cues for cell attachment, proliferation, and differentiation. This is crucial for ensuring the successful integration of the scaffold into the tissue regeneration process [27]. The mechanical properties of the cellular microenvironment, particularly scaffold stiffness, play a pivotal role in cell behavior regulation via mechanotransduction pathways [28]. Cells are highly responsive to the stiffness of their surroundings, which critically influences differentiation [29] outcome [30]. For example, softer substrates (0.1–1 kPa) tend to favor neuronal differentiation [31], while medium stiffness substrates (10–100 kPa) promote the differentiation of mesenchymal stem cells (MSCs) into myoblasts [32,33]. In contrast, stiffer substrates (>100 kPa) encourage osteogenic differentiation [34]. Beyond differentiation, scaffold stiffness also impacts cell adhesion and proliferation, with stiffer environments generally enhancing these processes. However, excessively stiff scaffolds may induce cellular stress, impairing normal cell function. Therefore, optimal scaffold stiffness must closely match that of the target tissue

to enhance tissue regeneration outcomes [35,36]. Soft tissues like skin and muscle, with stiffness values between 0.5–50 kPa, demand elastic scaffolds that can accommodate the dynamic mechanical properties of these tissues. The reported stiffness in this study is recognized appropriate for HDF cells as they require a softer scaffold.

In addition, the stiffness of Fmoc-FF hydrogels were tunable [37] by changing various parameters such as solvent choice, peptide concentration, peptide sequence, and the inclusion of hybrid peptides [38–40]. In our study, an increase in peptide concentration to 10 % led to a significant enhancement in stiffness (10 Kpa), demonstrating that concentration is a key factor in tuning the mechanical properties of Fmoc-FF hydrogels. These results suggest that the adjustable stiffness of Fmoc-FF hydrogels can be tailored to meet the specific requirements of different tissue types, making them a versatile scaffold material for a range of tissue engineering applications [25].

3.2. Architecture of the hydrogels based on their solvents

To further investigate the self-assembly behavior of FF peptide fibers over time and in various solvents, we utilized scanning electron microscopy (SEM) to observe FF self-assembly formed in HFIP and DMSO at 1 hour and 24 h post-formation (Fig. 3). The SEM images show that in HFIP, FF nanofibers rapidly develop into a dense, interconnected network within the first hour, which becomes even more compact by 24 h. Conversely, the DMSO-based structure, does not show fiber networks at the 1-hour mark; instead, it forms crystal-like rods. Unlike the entangled fiber structure seen in HFIP, the DMSO self-assembly lacks a similar fiber network, suggesting that the solvent significantly impacts the assembly rate, fiber density, and network architecture. Additionally, the SEM images validate the rheological findings, as DMSO gels are less compact compared to those in HFIP. Fmoc-FF dissolves best in HFIP, which promotes a quicker and denser fiber self-assembly process.

3.3. Fmoc-FF support the growth and viability of 3D encapsulated aHDF

First HDF were seeded in Fmoc-FF peptide hydrogels using 2D and 3D techniques and their viability and morphology was studied. This step was done to understand how the hydrogel stiffness and porosity effects HDF. In surface-coated hydrogel, peptide hydrogel is coated on the petri dish, and cells are seeded on top (2D cell culture). In the “Overlay Hydrogel” approach, peptide hydrogel is coated on top of the seeded cells (2D cell culture). In the “Infused Hydrogel”, cells are infused within the peptide hydrogel (3D cell culture). The infused hydrogel was kept in cell inserts and the surrounding medium was exchanged.

The surface-coated hydrogel showed similar cell viability comparable to the control, while the overlay and infused hydrogels demonstrated the highest viability among the samples (Fig. 4). Staining the live/dead cells confirmed these results, with the HDF cells forming a dense, spread layer in the overlay hydrogels (Fig. 4). The results indicate that the surface-coated hydrogel supported cell viability comparable to the control, however, the cells exhibited a different morphology, due to varying surface properties influencing cell behavior. Additionally, the number of dead cells in the cell-laden hydrogels was lower compared to the control. The overlay hydrogels, which had the highest viability, suggest that this configuration provided a more favorable environment for cell attachment, proliferation, and

survival. The dense and spread layer of HDF cells observed in the overlay hydrogels points to enhanced cell-matrix interactions, which may have promoted better cell distribution and function. While in the overlay approach, HDF are in 2D layer and Fmoc-FF is seeded on top of the cells. We suggest that the hydrogel has provided sufficient mechanical cues or adhesive ligands necessary for the cells to fully spread and align their typical fibroblast morphology.

3.4. Cell morphology in encapsulated remains as spheres

HDF exhibited distinct morphologies when seeded on various samples providing valuable information on how cells interact with peptide in 2D and 3D layers (Fig. 5). In control, cells displayed a spread attachment, and proliferation which is a typical morphology of HDF. In surface coated hydrogel, which cells were seeded in 2D layers on peptide coated surfaces, cells showed a round sphere morphology. In the overlay hydrogel, where Fmoc-FF hydrogel is seeded on top of cells, exhibited dense layers of aligned and stretched HDF. HDF (human dermal fibroblast) cells encapsulated within Fmoc-FF gels predominantly exhibited a thin spherical morphology. Previous studies have demonstrated that cell spreading is dependent on the balance between matrix stiffness and the availability of cell-adhesive ligands, with soft, non-adhesive matrices generally promoting a rounded, non-spread morphology [1]. Both spread-out and spherical cell morphologies offer distinct advantages in tissue engineering, depending on the tissue type. Spread-out morphology is ideal for scaffolds designed to mimic tissues like skin, bone, or muscle, where cell adhesion, ECM production, and migration are crucial for tissue repair and integration. The findings from this work indicate that the 2D peptide overlay directs cells to stretch and align, significantly compared to control cells, potentially enhancing their differentiation capabilities. In contrast, spherical morphology is beneficial for scaffolds that rely on cell-cell interactions, such as those used in cartilage or organoid formation, where spherical cell aggregates promote enhanced tissue formation and differentiation. The spherical morphology observed in the Fmoc-FF gels suggests that the hydrogel provides a microenvironment conducive to maintaining cellular integrity without promoting excessive adhesion.

This is particularly useful in applications, where maintaining a more quiescent, rounded state can prevent excessive cell spreading, which might otherwise lead to premature differentiation or cellular exhaustion. Additionally, spherical cell aggregates, such as spheroids, are known to enhance cell-cell communication [41], promote the deposition of extracellular matrix, and support a more in vivo-like phenotype [42], all of which are essential for tissue formation. The spherical shape of HDF cells could also facilitate the creation of multicellular spheroids or organoid-like structures, which have been shown to improve the efficiency of tissue regeneration by more closely mimicking the 3D architecture and behavior of cells in vivo. These cell aggregates often exhibit enhanced functionality, with better retention of stemness, improved differentiation potential, and increased secretion of extracellular matrix proteins, which are critical for the development of new tissue. Adjustments, such as incorporating cell-adhesive peptides (e.g., RGD) or modulating the stiffness and porosity of the gel, could encourage a more favorable interaction between the cells and the hydrogel matrix, promoting cell spreading and function.

3.5. Cell attachment and proliferation is enhanced with modified hybrid PEGDA

We printed 3D lumen with unmodified PEGDA and hybrid PEGDA/peptide bioinks (Fig. 6A, B). The process begins with a CAD file, which the onboard software converts into a series of 2D images. These images are then projected using visible light onto a vat of Photoink™ hydrogel [12], specifically optimized by volumetric for DLP bioprinting. The exposed regions of the hydrogel undergo crosslinking and solidification to form a single layer. The build platform then moves upward, allowing the light to cure successive image slices until the complete 3D structure is formed.

Peptide were either infused in the ink or were coated on the PEGDA after printing. HDF cells did not attach to unmodified PEGDA, which confirms that PEGDA alone is not a suitable ink to support cell adhesion and growth. Using the hybrid PEGDA/peptide bioink, cells predominantly adhered to the lumens, highlighting the critical role of peptides in initiating cell growth. The cells were mainly attached to the porous parts of the lattice suggesting the role of porosity in supporting (Fig 6B) cell growth [43]. After 24 h of seeding, HDF cells exhibited a spreading morphology (Fig. 6D). The live and dead cells seeded on the different PEGDA lumens are presented in Fig. 7. Matrigel-coated lumens were used as a control. While HDF cells proliferated and spread on the Matrigel-coated PEGDA, the rapid degradation, challenging handling conditions, and structural loss of Matrigel present significant limitations for long-term applications.

The peptide-coated lumens successfully supported cell growth, with the majority of cells remaining viable and only a few dead cells observed (Fig. 7). Studying the cell morphology revealed that the cytoplasmic actins of HDF cells seeded on PEGDA/peptide lumens were significantly spread, a sign of active cytoskeletal rearrangement (Fig. 8) [44]. This spreading morphology is indicative of the initiation of differentiation, as cell spreading is often associated with increased cell-ECM interactions and mechanical signals that trigger differentiation pathways [44].

Previous studies have also demonstrated that Fmoc-FF enhances the differentiation of mesenchymal stem cells (MSCs) [23]. Similarly, in our study, we observed that the PEGDA/peptide bioinks promoted the spreading of F-actin filaments and robust cell-ECM interactions. The ability of these bioinks to encourage differentiation is crucial for tissue engineering applications, where scaffold design must support not only cell viability but also appropriate mechanical and biochemical cues to guide cell fate. The spread morphology seen in our results aligns with the mechanical stimuli needed to enhance cell adhesion, signaling pathways, and ultimately, differentiation, making the PEGDA/peptide bioinks a promising tool for creating functional tissue scaffolds.

4. Conclusion

The development of hybrid PEGDA/peptide bioinks has shown significant promise in overcoming the limitations of traditional PEGDA bioinks, particularly in supporting cell adhesion and proliferation providing cells with mechanical cues. The incorporation of Fmoc-FF peptides into PEGDA lumens enhances the bioactivity of the scaffold, enabling human dermal fibroblast (HDF) cells to attach, proliferate, and exhibit a spread morphology. The

tunable stiffness of the hybrid scaffolds, ranging from 100 Pa to 10 kPa, is crucial for addressing the mechanical requirements of various tissue types, including skin, cartilage, and bone. These findings demonstrate that peptide-modified bioinks offer a versatile platform for fabricating biocompatible, cell-laden scaffolds.

Acknowledgment

Research reported in this publication was supported by the National Institute of General Medical Science (NIGMS) of the National Institutes of Health under award number R16GM150848.

References

[1]. Zhu W, Ma X, Gou M, Mei D, Zhang K, Chen S, 3D printing of functional biomaterials for tissue engineering, Curr. Opin. Biotechnol 40 (2016) 103–112, 10.1016/j.copbio.2016.03.014. Aug. [PubMed: 27043763]

[2]. Ma Y, Deng B, He R, Huang P Advancements of 3D bioprinting in regenerative medicine: exploring cell sources for organ fabrication, Heliyon 10 (3) (2024) e24593, 10.1016/j-heliyon.2024.e24593. Feb. [PubMed: 38318070]

[3]. Li Y, et al. , 3D embedded bioprinting of large-scale intestine with complex structural organization and blood capillaries, Biofabrication 16 (4) (2024) 045001, 10.1088/1758-5090/ad5b1b. Oct.

[4]. Zhang YS, et al. , 3D extrusion bioprinting, Nat. Rev. Methods Prim 1 (1) (2021) 75, 10.1038/s43586-021-00073-8. Nov.

[5]. Ramesh S, et al. , Extrusion bioprinting: recent progress, challenges, and future opportunities, Bioprinting 21 (2021) e00116, 10.1016/j.bprint.2020.e00116. Mar.

[6]. Do A, Khorsand B, Geary SM, Salem AK, 3D Printing of scaffolds for tissue regeneration applications, Adv. Healthc. Mater 4 (12) (2015) 1742–1762, 10.1002/adhm.201500168. Aug. [PubMed: 26097108]

[7]. Gopinathan J, Noh I, Recent trends in bioinks for 3D printing, Biomater. Res 22 (1) (2018), 10.1186/s40824-018-0122-1. Dec.

[8]. Zheng Z, Eglin D, Alini M, Richards GR, Qin L, Lai Y, Visible light-induced 3D bioprinting technologies and corresponding bioink materials for tissue engineering: a review, Engineering 7 (7) (2021) 966–978, 10.1016/j.eng.2020.05.021. Jul.

[9]. Elkhoury K, Zuazola J, Vijayavenkataraman S, Bioprinting the future using light: a review on photocrosslinking reactions, photoreactive groups, and photoinitiators, SLAS. Technol 28 (3) (2023) 142–151, 10.1016/j.slast.2023.02.003. Jun. [PubMed: 36804176]

[10]. Zhou X, et al. , 3D bioprinting-tunable small-diameter blood vessels with biomimetic biphasic cell layers, ACS. Appl. Mater. Interfaces 12 (41) (2020) 45904–45915, 10.1021/acsami.0c14871. Oct. [PubMed: 33006880]

[11]. Cao X, Maharjan S, Ashfaq R, Shin J, Zhang YS, Bioprinting of small-diameter blood vessels, Engineering 7 (6) (2021) 832–844, 10.1016/j.eng.2020.03.019. Jun.

[12]. Levato R, et al. , Light-based vat-polymerization bioprinting, Nat. Rev. Methods Prim 3 (1) (2023) 47, 10.1038/s43586-023-00231-0.Jun.

[13]. Mirshafiei M, Rashedi H, Yazdian F, Rahdar A, Baino F, Advancements in tissue and organ 3D bioprinting: current techniques, applications, and future perspectives, Mater. Des 240 (2024) 112853, 10.1016/j.matdes.2024.112853. Apr.

[14]. Ashammakhi N, et al. , Bioinks and bioprinting technologies to make heterogeneous and biomimetic tissue constructs, Mater. Today. Bio 1 (2019) 100008, 10.1016/j.mtbio.2019.100008. Jan.

[15]. Bose S, Vahabzadeh S, Bandyopadhyay A, Bone tissue engineering using 3D printing, Mater. Today 16 (12) (2013) 496–504, 10.1016/j.mattod.2013.11.017. Dec.

[16]. Evangelista M, et al. , Single-lumen and multi-lumen Poly(Ethylene Glycol) nerve conduits fabricated by stereolithography for peripheral nerve regeneration in vivo, J. Reconstr. Microsurg 31 (05) (2015) 327–335, 10.1055/s-0034-1395415. Apr. [PubMed: 25893632]

[17]. Sheng L, Li M, Zheng S, Qi J, Adjusting the accuracy of PEGDA-GelMA vascular network by dark pigments via digital light processing printing, J. Biomater. Appl 36 (7) (2022) 1173–1187, 10.1177/08853282211053081. Feb. [PubMed: 34738507]

[18]. Marchioli G, et al. , Layered PEGDA hydrogel for islet of Langerhans encapsulation and improvement of vascularization, J. Mater. Sci. Mater. Med 28 (12) (2017) 195, 10.1007/s10856-017-6004-6. Dec. [PubMed: 29151130]

[19]. Almubarak S, et al. , Tissue engineering strategies for promoting vascularized bone regeneration, Bone 83 (2016) 197–209, 10.1016/j.bone.2015.11.011. Feb. [PubMed: 26608518]

[20]. Zadeh Moslabeh FG, Miar S, Habibi N, In vitro self-assembly of a modified diphenylalanine peptide to nanofibers induced by the eye absent enzyme and alkaline phosphatase and its activity against breast cancer cell proliferation, ACS. Appl. Bio. Mater 6 (1) (2023) 164–170, 10.1021/acsabm.2c00829. Jan.

[21]. Fouladgar F, et al. , Mesenchymal stem cells aligned and stretched in self-assembling peptide hydrogels, Heliyon 10 (1) (2024) e23953, 10.1016/j.heliyon.2023.e23953. Jan. [PubMed: 38234902]

[22]. Zhou M, et al. , Self-assembled peptide-based hydrogels as scaffolds for anchorage-dependent cells, Biomaterials 30 (13) (2009) 2523–2530, 10.1016/j.biomaterials.2009.01.010. May. [PubMed: 19201459]

[23]. Wang Y, et al. , Self-assembled peptide-based hydrogels as scaffolds for proliferation and multi-differentiation of mesenchymal stem cells, Macromol. Biosci 17 (4) (2017), 10.1002/mabi.201600192. Apr.

[24]. Kumar P, Nagarajan A, Uchil PD, Analysis of Cell Viability by the MTT Assay, Cold. Spring. Harb. Protoc 2018 (6) (2018), 10.1101/pdb.prot095505 pdb.prot095505Jun.

[25]. Dudukovic NA, Zukoski CF, Mechanical properties of self-assembled fmoc-diphenylalanine molecular gels, Langmuir 30 (15) (2014) 4493–4500, 10.1021/la500589f. Apr. [PubMed: 24684510]

[26]. Fu Z, Naghieh S, Xu C, Wang C, Sun W, Chen X, Printability in extrusion bioprinting, Biofabrication 13 (3) (2021) 033001, 10.1088/1758-5090/abe7ab. Jul.

[27]. Janmey PA, Fletcher DA, Reinhart-King CA, Stiffness Sensing by Cells, Physiol. Rev 100 (2) (2020) 695–724, 10.1152/physrev.00013.2019. Apr. [PubMed: 31751165]

[28]. Wells RG, The role of matrix stiffness in regulating cell behavior, Hepatology 47 (4) (2008) 1394–1400, 10.1002/hep.22193. Jan. [PubMed: 18307210]

[29]. Lv H, et al. , Mechanism of regulation of stem cell differentiation by matrix stiffness, Stem. Cell. Res. Ther 6 (1) (2015) 103, 10.1186/s13287-015-0083-4. Dec. [PubMed: 26012510]

[30]. Chen J, et al. , Cell mechanics, structure, and function are regulated by the stiffness of the three-dimensional microenvironment, Biophys. J 103 (6) (2012) 1188–1197, 10.1016/j.bpj.2012.07.054. Sep. [PubMed: 22995491]

[31]. Stukel JM, Willits RK, The interplay of peptide affinity and scaffold stiffness on neuronal differentiation of neural stem cells, Biomed. Mater 13 (2) (2018) 024102, 10.1088/1748-605X/aa9a4b. Feb. [PubMed: 29133625]

[32]. Romanazzo S, et al. , Substrate stiffness affects skeletal myoblast differentiation in vitro, Sci. Technol. Adv. Mater 13 (6) (2012) 064211, 10.1088/1468-6996/13/6/064211. Dec. [PubMed: 27877538]

[33]. Levy-Mishali M, Zoldan J, Levenberg S, Effect of scaffold stiffness on myoblast differentiation, Tissue. Eng. Part. A 15 (4) (2009) 935–944, 10.1089/ten.tea.2008.0111. Apr. [PubMed: 18821844]

[34]. El-Rashidy AA, et al. , Effect of polymeric matrix stiffness on osteogenic differentiation of mesenchymal stem/progenitor cells: concise review, Polymers. (Basel) 13 (17) (2021) 2950, 10.3390/polym13172950. Aug. [PubMed: 34502988]

[35]. Breuls RGM, Jiya TU, Smit TH, Scaffold stiffness influences cell behavior: opportunities for skeletal tissue engineering, Open. Orthop. J 2 (1) (2008) 103–109, 10.2174/1874325000802010103. Jun. [PubMed: 19478934]

[36]. Irawan V, Sung T-C, Higuchi A, Ikoma T, Collagen scaffolds in cartilage tissue engineering and relevant approaches for future development, Tissue. Eng. Regen. Med 15 (6) (2018) 673–697, 10.1007/s13770-018-0135-9. Dec. [PubMed: 30603588]

[37]. Mohammed M, Lai T-S, Lin H-C, Substrate stiffness and sequence dependent bioactive peptide hydrogels influence the chondrogenic differentiation of human mesenchymal stem cells, J. Mater. Chem. B 9 (6) (2021) 1676–1685, 10.1039/D0TB02008G. [PubMed: 33491723]

[38]. Bairagi D, et al. , Self-assembling peptide-based hydrogel: regulation of mechanical stiffness and thermal stability and 3D cell culture of fibroblasts, ACS. Appl. Bio. Mater 2 (12) (2019) 5235–5244, 10.1021/acsabm.9b00424. Dec.

[39]. Hogrebe NJ, et al. , Independent control of matrix adhesiveness and stiffness within a 3D self-assembling peptide hydrogel, Acta. Biomater 70 (2018) 110–119, 10.1016/j.actbio.2018.01.031. Apr. [PubMed: 29410241]

[40]. Scelsi A, et al. , Tuning of hydrogel stiffness using a two-component peptide system for mammalian cell culture, J. Biomed. Mater. Res. A 107 (3) (2019) 535–544, 10.1002/jbm.a.36568. Mar. [PubMed: 30456777]

[41]. Arakawa H, Takeda K, Higashi SL, Shibata A, Kitamura Y, Ikeda M, Self-assembly and hydrogel formation ability of Fmoc-dipeptides comprising α-methyl-L-phenylalanine, Polym. J 52 (8) (2020) 923–930, 10.1038/s41428-019-0301-5. Aug.

[42]. Dado D, Levenberg S, Cell–scaffold mechanical interplay within engineered tissue, Semin. Cell. Dev. Biol 20 (6) (2009) 656–664, 10.1016/j.semcdb.2009.02.001. Aug. [PubMed: 19596326]

[43]. Jiang S, Li SC, Huang C, Chan BP, Du Y, Physical properties of implanted porous bioscaffolds regulate skin repair: focusing on mechanical and structural features, Adv. Healthc. Mater 7 (6) (2018), 10.1002/adhm.201700894. Mar.

[44]. Smith PG, Deng L, Fredberg JJ, and Maksym GN, “Mechanical strain increases cell stiffness through cytoskeletal filament reorganization,” Am. J. Physiol. Lung. Cellul. Mole. Physiol, vol. 285, no. 2, pp. L456–L463, Aug. 2003, doi: 10.1152/ajplung.00329.2002.

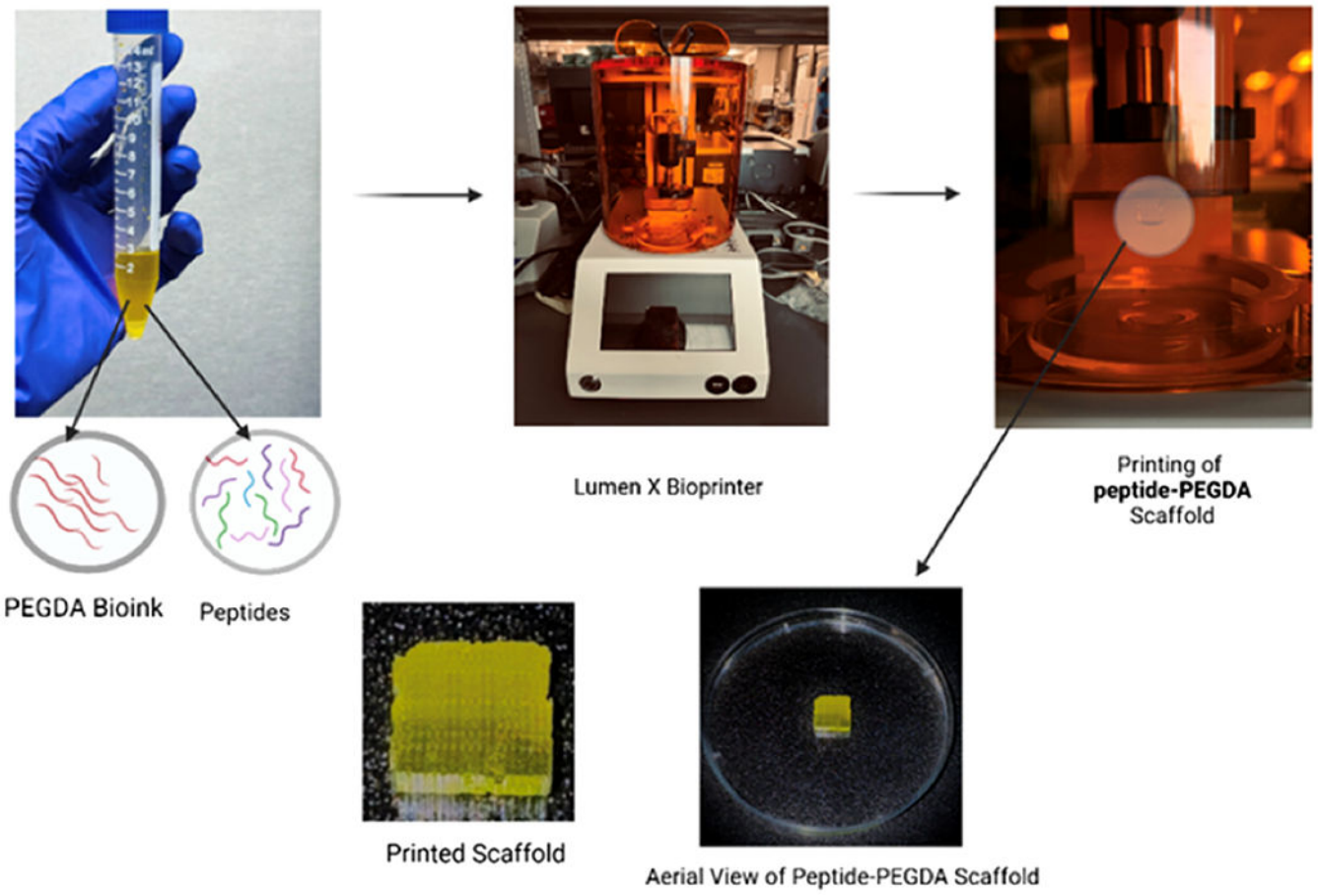

Fig. 1.
Schematic overview of 3D printing Lumens with PEGDA/peptide bioinks.

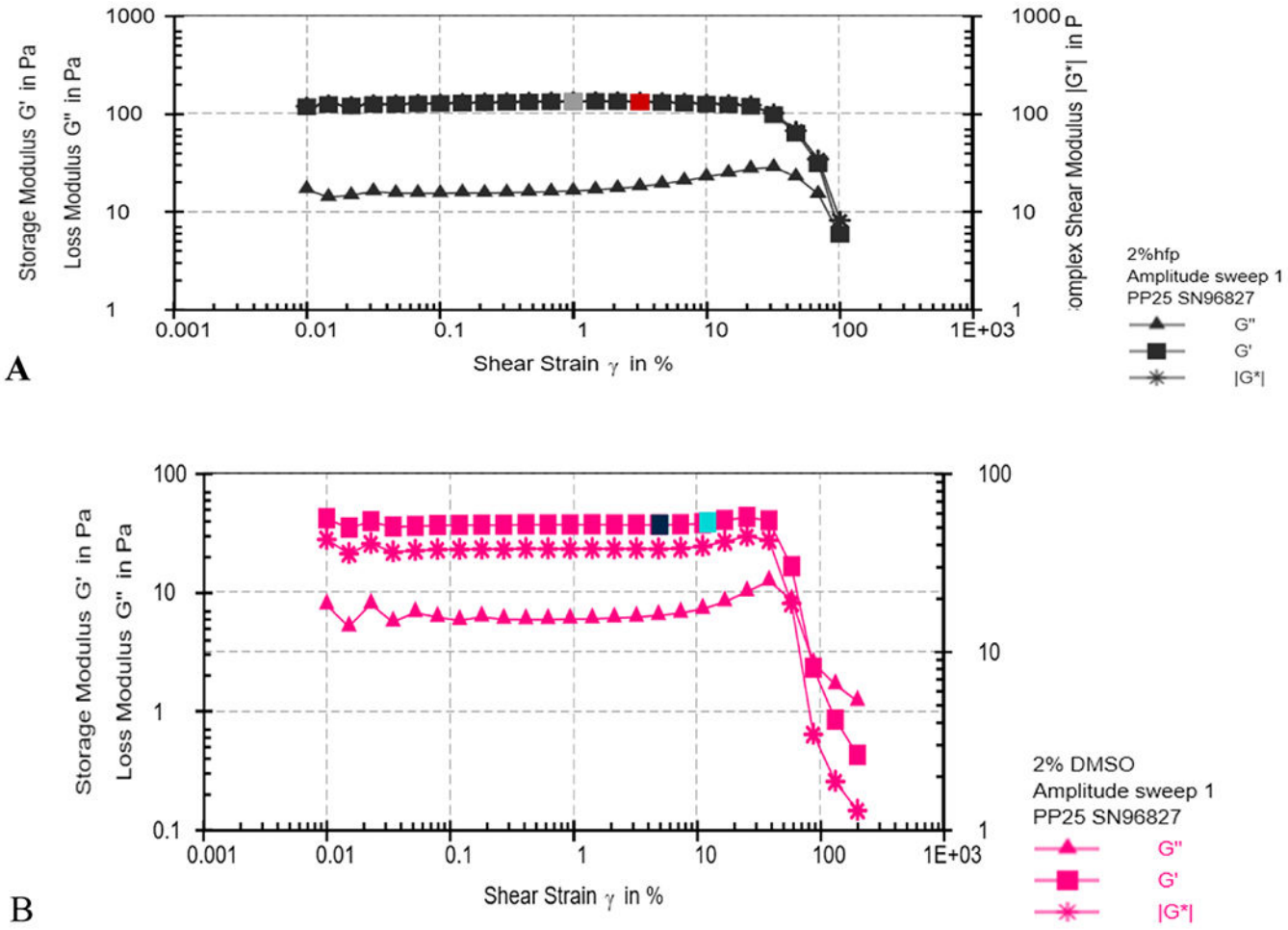

Fig. 2.

Storage Modulus (G') and Loss modulus (G") of a) 2 % Fmoc-FF in HFP; b) 2 % Fmoc-FF in DMSO.

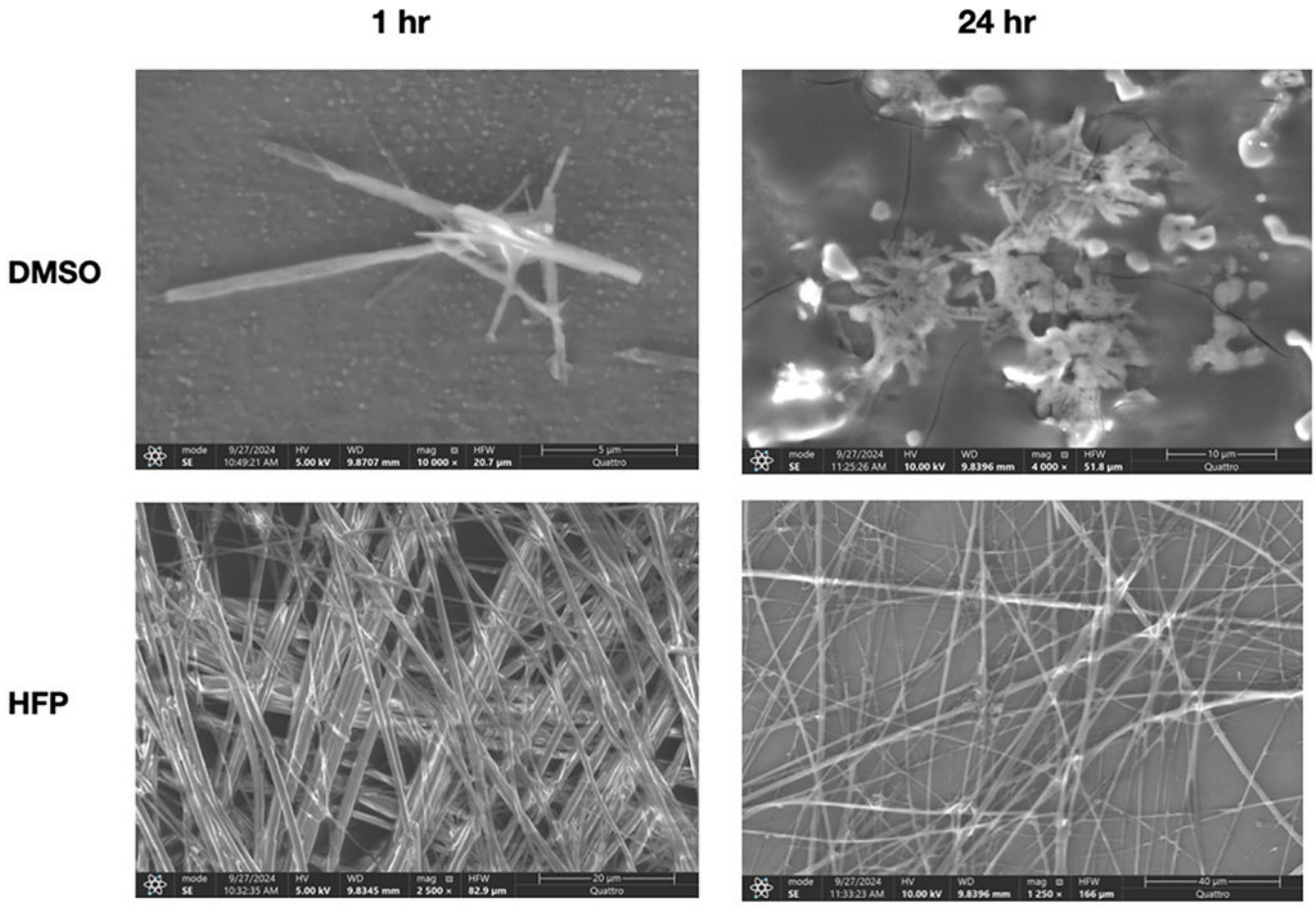

Fig. 3.
SEM image of FF in HFP and DMSO after 1 hr and 24 hr.

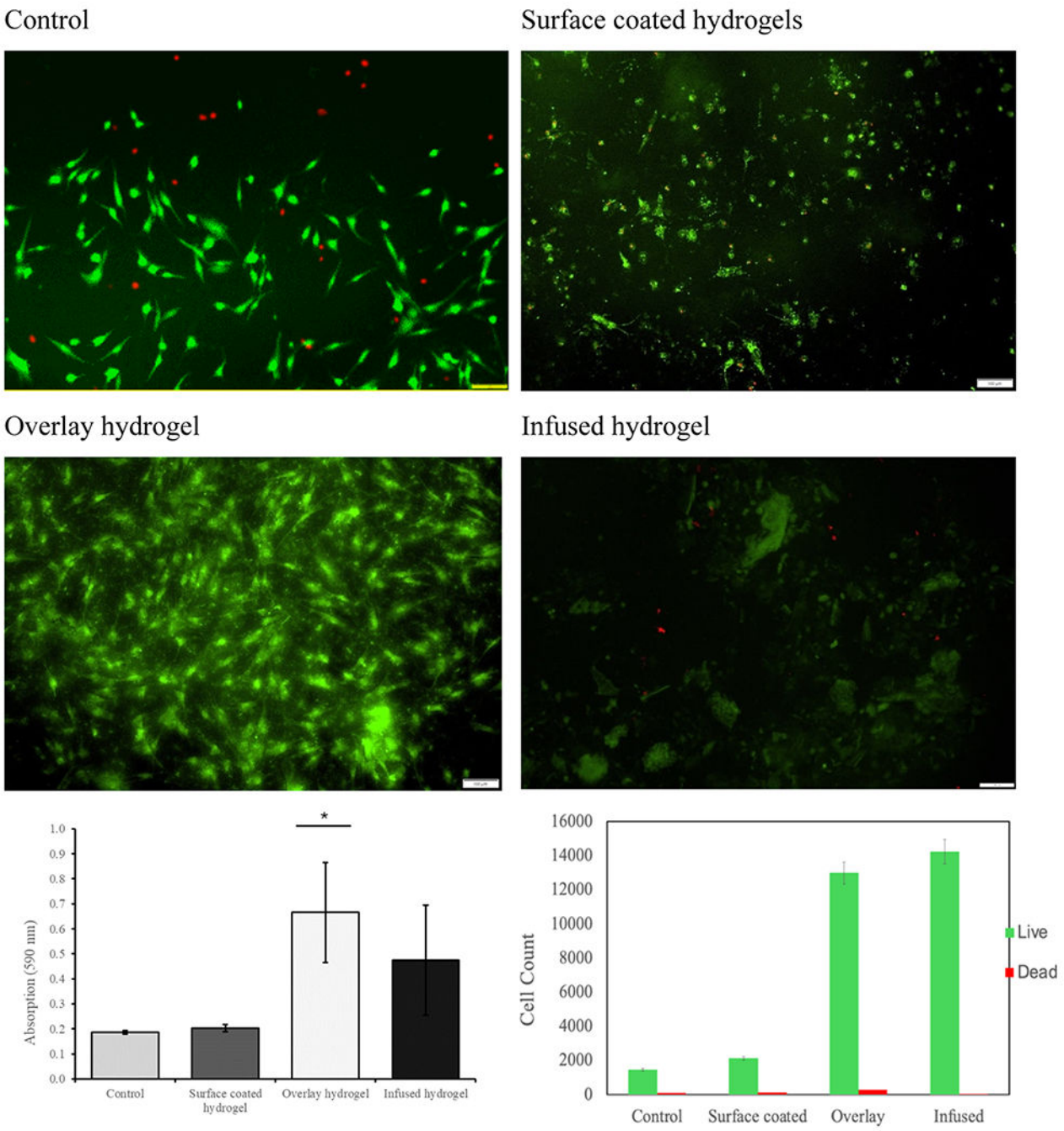

Fig. 4.

Live (green) and dead (red) staining of different cell-laden of human dermal fibroblast with Fmoc-FF hydrogels. Surface-Coated Hydrogel: Peptide hydrogel is coated on the petri dish, and cells are seeded on top (2D cell culture). Overlay hydrogel: Peptide hydrogel is coated on top of the seeded cells (2D cell culture). Infused hydrogel: Cells are infused within the peptide hydrogel (3D cell culture) scale bar=100μm. MTT viability of HDF in different cell-laden hydrogels. Graph of live and dead cell count processed with ImageJ.

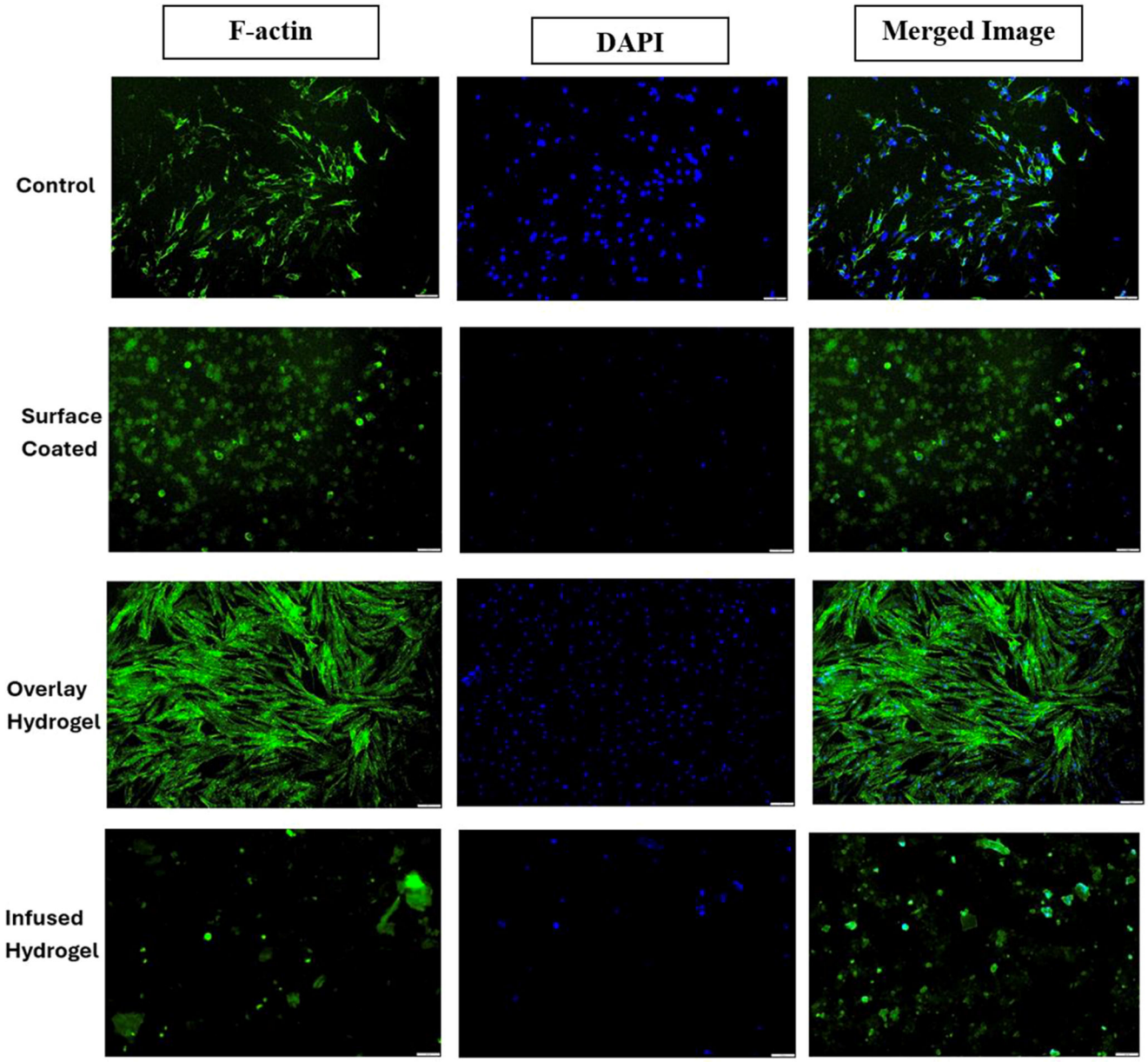

Fig. 5.

F-actin cytoplasm (green) and DAPI nucleus (blue) staining of different cell-laden of human dermal fibroblast with Fmoc-FF hydrogels. Surface-Coated Hydrogel: Peptide hydrogel is coated on the petri dish, and cells are seeded on top (2D cell culture). Overlay hydrogel: Peptide hydrogel is coated on top of the seeded cells (2D cell culture). Infused hydrogel: Cells are infused within the peptide hydrogel (3D cell culture) (scale bar, 100 μm).

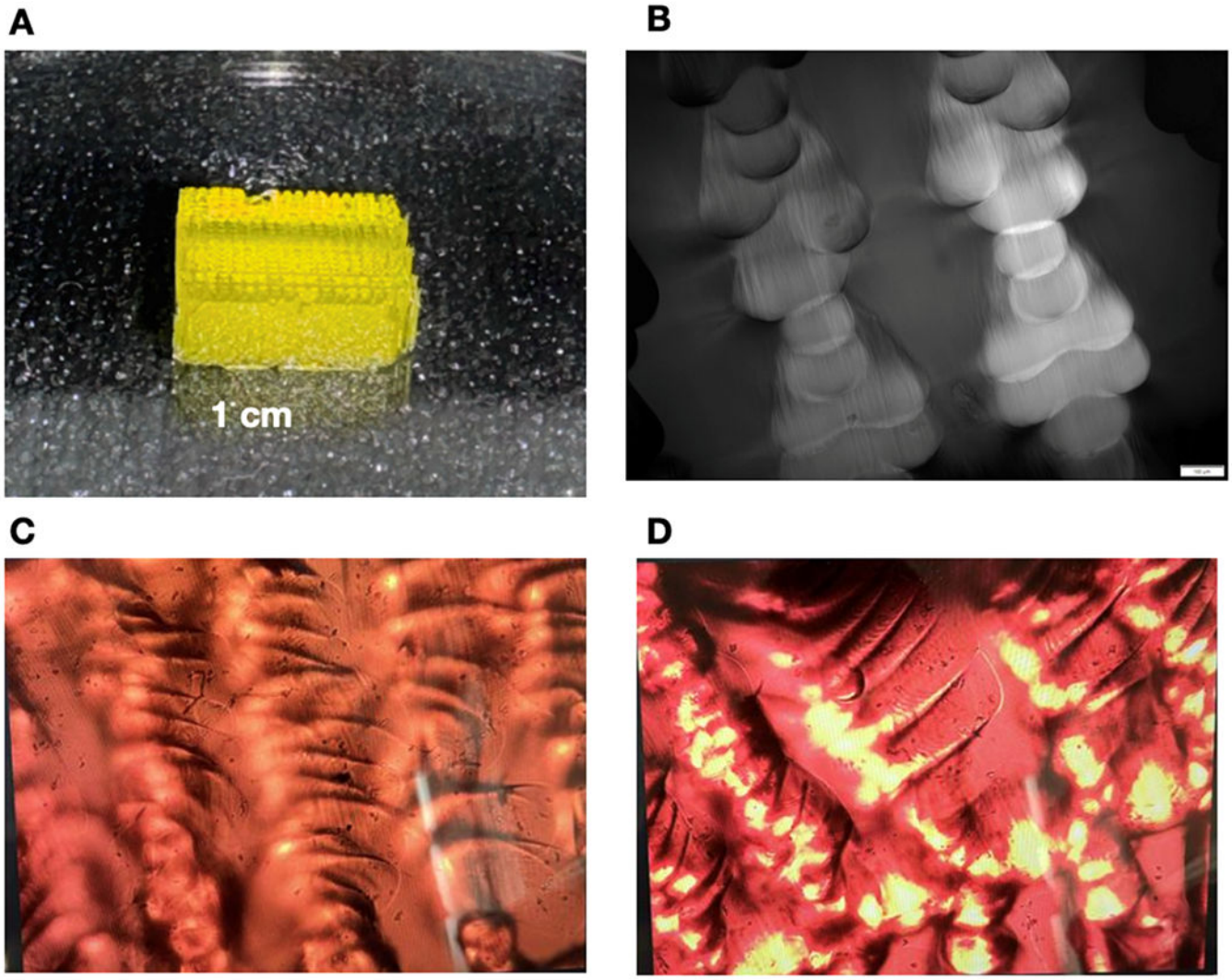

Fig. 6.
3D printed lumens, B) Bright field of lumens without cells, C) HDF cells seeded in lumens after 1 hr, D) after 24 hr.

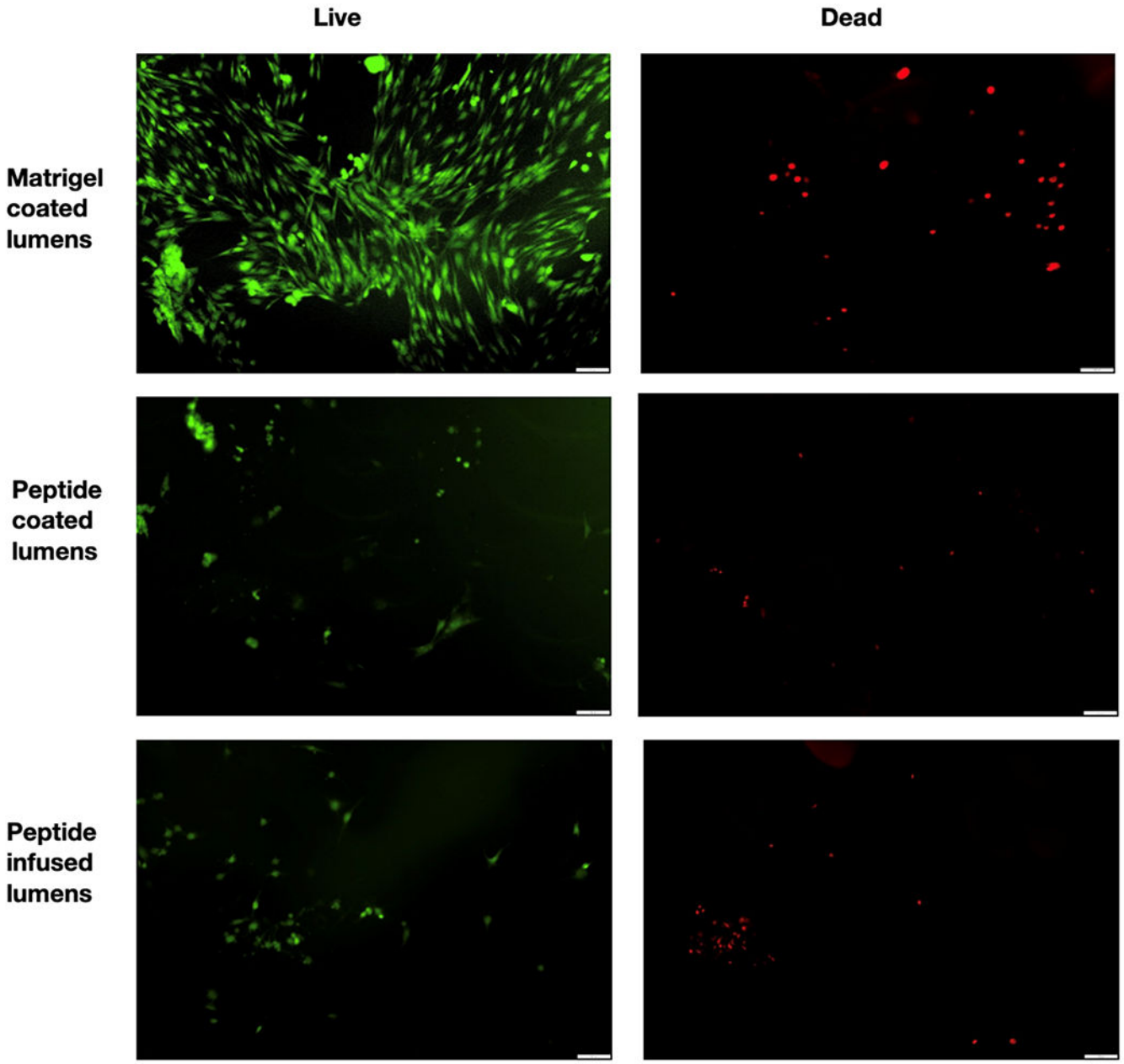

Fig. 7.
Live (green) and dead (red) cells of HDF seeded on Matrigel coated, peptide coated and peptide infused lumens (scale bar, 100 μm).

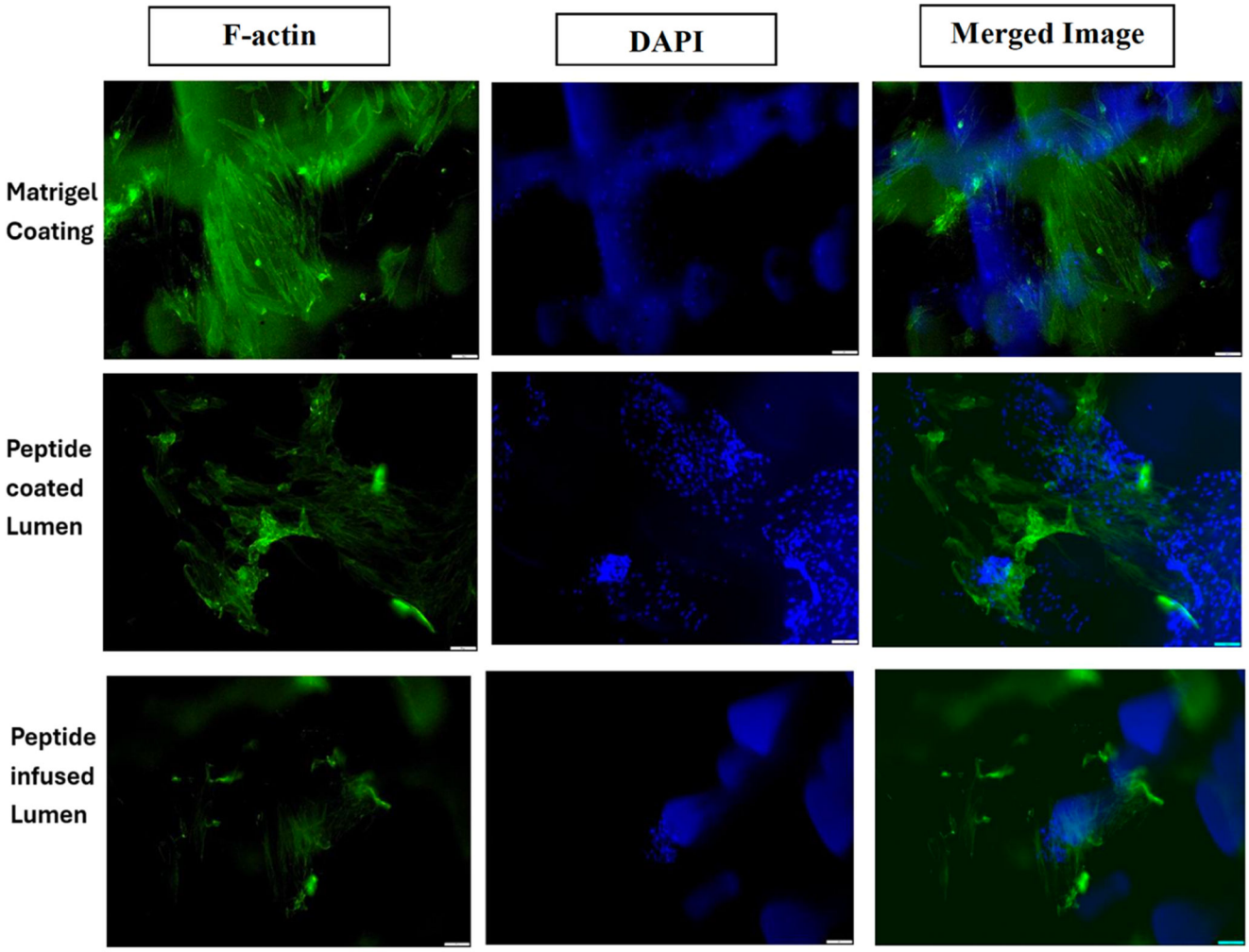

Fig. 8.
F-actin cytoplasm (green) and nucleus (blue) of peptide coated and peptide infused lumens (scale bar, 100 μm).